OPTICAL MEASUREMENTS OF THE OUTER SCALE OF THE ATMOSPHERIC TURBULENCE

V.P. Lukin

Institute of Atmospheric Optics,
Siberian Branch of the Russian Academy of Sciences, Tomsk
Received January 14, 1992

On the basis of generalization of numerous measurement the low—frequency range of the turbulence spectrum of the atmosphere, adjacent to the inertial range is analyzed. The turbulence spectra are compared with the isotropic models.

In the surface layer of the atmosphere the outer scale of the atmospheric turbulence depends not only on the altitude above the underlying surface but also on the atmospheric stratification.

1. RECONSTRUCTION OF THE SPECTRAL POWER DENSITY OF THE FLUCTUATIONS OF THE REFRACTIVE INDEX FROM THE OPTICAL MEASUREMENTS

Light scattering on the turbulent inhomogeneities of the atmosphere is one of the main mechanisms of distortion of the received optical signal. The random spatio—temporal variations in the refractive index of the atmosphere[1] result in the distortion of the optical beam structure, intensity, and phase fluctuations of optical waves and are manifested, in particular, in blurring, jittering, and scintillating of the source images as well as in the turbulent extinction of the average received power of the signal.

At the same time, investigation of these fluctuations has entailed the development of the methods for the remote sensing of the atmospheric turbulence. Laser sensing of the atmospheric turbulence develops intensively since the application of lasers for measuring of the parameters of the atmospheric turbulence has a number of advantages. In particular, the optical measurements ensure higher stability and reliability of the obtained statistical data, since the characteristics being determined are additionally averaged over the propagation path.

The light wave propagating through the medium with the inhomogeneities of the refractive index undergoes distortions of its parameters.[2] These distortions can be used for determining the characteristics of the inhomogeneities. Measurements can be performed remotely without insertion of the measuring sensor at the point being investigated, do not disturb the medium being studied, and allow one to investigate the media in which the sensors cannot be placed.

A number of problems arises when we try to relate the measurements of the fluctuations of the parameters of optical wave propagated through the atmospheric layer with the atmospheric parameters. First, the relation between the atmospheric parameters of interest and the experimental data in the form of the equation must be found. Second, the convenient mathematical apparatus for retrieval of the information about the atmosphere from the experimental data is needed. This problem is far from being trivial, since the measured quantities are often related with the atmospheric parameters by the integral equations. Thus, the problem is to solve the integral equations. The analytic solutions of these equations can be found only for the particular cases from those of interest for us and, as a rule, numerical methods must be used. And, finally, the measurements must be sufficiently complete and accurate.

The most developed method for measuring the power spectrum of the fluctuation of the refractive index is the method of its reconstruction from the measured fluctuations statistical characteristics of the parameters of optical waves propagated through the turbulent atmospheric layer. In the case of propagation of optical waves through the turbulent atmosphere in which the relative fluctuations of the refractive index are weak and variations in the refractive index at distances of the order of wavelength are also small the power spectra of fluctuations of the refractive index of the medium can be determined from the spectra and correlation functions for the fluctuation characteristics of optical waves.[3]

It should be kept in mind that the temperature turbulence and similarity of the spectra of fluctuations of the refractive index and temperature are practically always considered for optical waves.

When studying the atmospheric turbulence spectra by the optical methods, the question arises about the sensitivity of the measured parameters of optical waves to the functional form of the spectral power density of the fluctuations of the refractive index $\Phi_n(\kappa)$. The problem is to choose such a characteristic of the optical wave, which will provide for the simplicity of experimental measurements and will be extremely sensitive to the form of the spectrum $\Phi_n(\kappa)$ in either of its spectral region.

The atmospheric turbulence spectrum even in the surface layer is characterized by a wide dynamic range (the spatial scales vary from several meters up to several parts of millimeter) and, in view of the finite accuracy of optical measurements, cannot be reconstructed from the measurements of fluctuations of a single parameter of an optical wave. Investigations of the sensitivity of different parameters of optical waves to the form of the turbulence spectrum in different regions showed that the parameters related with the phase of the optical wave are primarily determined by the low—frequency inhomogeneities of the fluctuations of the refractive index, whereas the intensity fluctuations of optical radiation are determined by the high—frequency range of the turbulence spectrum.[3] In other words, measurements of the phase fluctuations of optical wave can be used for investigation of the energy range of turbulence spectrum while measurements of the the intensity fluctuations can be used for investigation of the equilibrium range incorporating the inertial and viscous ranges of turbulence spectrum.

1.1. Phase optical measurements of the fluctuations of the refractive index

Measuring the intensity fluctuations of optical radiation is a simpler problem comparing with measurements of the phase fluctuations. Therefore, reconstruction of the turbulence spectrum from the data of optical measurements were performed for the first time when measuring just the intensity fluctuations.[4] The turbulence spectrum was reconstructed in the dissipation range.

Phase measurements in the atmosphere in a wide dynamic range are complicated engineering problem.[5] Quite accurate experimental data on the behavior of the structure function of an optical wave at observation distances compared with the altitude of the near-ground atmospheric path were first obtained in Refs. 6 and 7. These data as well as the correlation functions of the fluctuations of the position of the centers[8,9] of the optical beams separated in the horizontal direction contradicted to the available theoretical calculations[10,11] obtained with the help of the Kolmogorov–Obukhov power-law model for the spectral power density of the fluctuation of the refractive index. The attempts of calculations[7,9,11] of these fluctuation characteristics of optical waves with the use of the isotropic models of the spectral power density are well known. These models take into account the deviation of the spectrum from the power-law dependence in the region of the outer scale of the turbulence. However, the degree of the reliability of the employed spectral models remains uncertain.
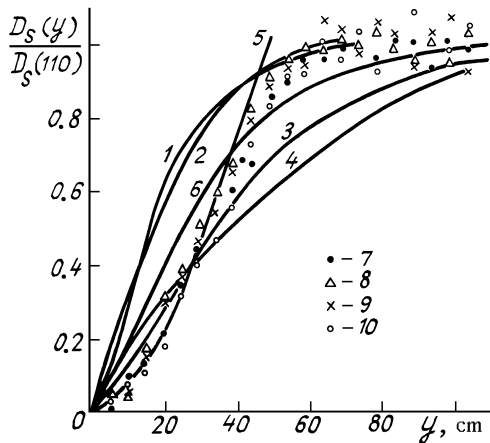

FIG. 1. The normalized phase structure functions. 1 and 3) calculations from formula (2) on the basis of model spectrum (6): 1) $\kappa_{01} = 6.5$ m^{-1} and 3) $\kappa_{01} = 3.2$ m^{-1}; 2 and 4) calculations from formula (26) on the basis of spectrum (21): 2) $\kappa_{02} = 26.5$ m^{-1} and 4) $\kappa_{02} = 11.8$ m^{-1}; 5) function $ay^{5/3}$, where a was chosen against the criterion of the best agreement with the experimental data; 6) calculation from formula (25) for $\kappa_{01} = 4.3$ m^{-1}; and, 7–10) experimental data.

In this section we discuss the results of the reconstruction of a two-dimensional fluctuation spectrum of the refractive index obtained from the experimental data on the phase structure function in Ref. 12. The experiment was performed in the atmosphere on the 110 m horizontal path. The altitude of the path above the underlying surface was 1.5 m. The radiation of a He–Ne laser was splitted to form two identically collimated beams 2 cm in diameter. The distance between the beams varied successively along the Y axis with

step $\Delta_y = 0.05$ m up to $y_m = 1.1$ m. The phase difference fluctuations between the beam centers were recorded in the receiving plane with the help of an optical digital phase meter.[5] Realizations of the phase differences over a period $T = 50$ s (the length of sequence was 5000 readings) were used for estimating the phase structure function $D_s(y)$. The structure functions normalized to their values at maximum separation $D_s(y_m)$, are shown in Fig. 1 for four runs of measurements. It can be seen that the structure functions saturate at a constant level. Therefore, in the framework of the hypothesis of "frozen" turbulence[10] for the scales $y \lesssim v_\perp T$ ($v_\perp$ is the wind velocity component in the direction transverse to the path, in this experiment $v_\perp \approx 2$ m/s) the phase fluctuations can be considered to be uniform.

Let us use the relation

$$\hat{b}_s(y) = \begin{cases} 1 - D_s(y)/D_s(y_m), & y \le y_m, \\ 0, & y > y_m \end{cases} \qquad (1)$$

as the estimate of the correlation coefficient of the phase fluctuations. If we perform the calculation of the correlation function for the phase fluctuations[12] $B_s(y)$ in the first approximation of the smooth perturbation method,[10] we will show that

$$B_s(y) = \int_{-\infty}^{+\infty} d\kappa_2 V_s(\kappa_2) \exp(i\kappa_2 y) \qquad , \qquad (2)$$

where

$$V_s(\kappa_2) = \int_{-\infty}^{+\infty} d\kappa_3 f_s(\kappa_2, \kappa_3) \Phi_n(0, \kappa_2, \kappa_3) . \qquad (3)$$

As the estimates showed, the spectral filtering function $f_s(\kappa_2, \kappa_3)$ can be assumed practically as constant. Then the one-dimensional phase spectrum $V_s(\kappa_2)$ will coincide with a two-dimensional spectrum of the fluctuations of the refractive index

$$V_n(0, \kappa_2) = \int_{-\infty}^{+\infty} d\kappa_3 \Phi_n(0, \kappa_2, \kappa_3) \qquad (4)$$

to within a constant factor. Thus, we can determine the two-dimensional spectrum (4) from the measured values of the correlation coefficient given by Eq. (1).

According to Ref. 13, the Fourier transform of the experimental correlation functions $\hat{b}(y)$ can be calculated from the formula

$$\overline{v}_s(\kappa_2) = \frac{\Delta_y}{\pi} \left[1 + 2 \sum_{k=1}^{i-1} \hat{b}_s(y_k) \, \omega(y_k) \cos(k_2 y_k) \right] , \qquad (5)$$

$$\omega(y_k) = \begin{cases} 1 - 6(|U|/M)^2 - 6(|U|/M)^3, & |U| \le M/2, \\ 2(1 - |U|/M)^3, & M/2 < |U| \le M, \\ 0, & |U| > M . \end{cases}$$

where $y_k = k\Delta_y$, $\overline{v}(\kappa_2) = v_s(\kappa_2)/\sigma_s^2$ is the normalized spectrum, and σ_s^2 is the variance of the phase fluctuations, $\omega(U)$ is Parson's correlation window, and $M = l\Delta_y$ is the width of the correlation window ($M = 1.1$ m). The spectra

$\overline{v}_s(\kappa_2)$ calculated from the experimental data (Fig. 1) are shown in Fig. 2. The 80% confidence level is shown by the vertical bar.
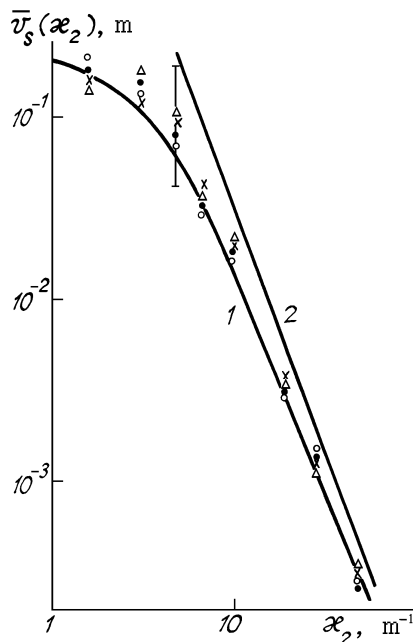

FIG. 2. *The spectrum of the fluctuation of the refractive indices: 1 and 2) model spectrum (6) and (4) and asymptote of this spectrum for κ_{01} = 4.3 m^{-1}, respectively. Designation of the experimental points corresponds to Fig. 1.*

Let us compare the experimental data with the results of calculations performed on the basis of the isotropic model of the spectrum $\Phi_n(0, \kappa_2, \kappa_3)$ in the region of the outer scale of the turbulence

$$\Phi_n(0, \kappa_2, \kappa_3) = 0.033C_n^2\left(\kappa_0^2 + \kappa_2^2 + \kappa_3^2\right)^{-11/6}, \qquad (6)$$

here $\kappa_0 = 2\pi/L_0$ is the wave number corresponding to the outer scale of the turbulence L_0 and C_n^2 is the structure parameter[10] of the refractive index. Substituting the model described by Eq. (6) into Eqs. (3) and (4) we obtain that for this experiment

$$V_s(\kappa_2) = 2\pi k^2 L V_n(0, \kappa_2),$$

where $k = 2\pi/\lambda$, λ is the radiation wavelength, and L is the path length (110 m). Comparison between experimental spectra (5) and the model spectra given by Eq. (3) is shown in Fig. 2. The outer scale of model spectrum (6) was $\kappa_0 = 4.3$ m^{-1} and was chosen from the condition of agreement with the experimental data at maximum frequency. The normalized structure function corresponding to this spectrum is shown in Fig. 1 (curve *1*) while curve *2* of this figure corresponds to the Kolmogorov–Obykhov model. As can be seen from Figs. 1 and 2, the spectra and the structure functions, on the whole, correspond to model (6), however deviation of the experimental functions from the power–law dependences (curves *2* in Figs. 1 and 2) takes place for lower spatial frequencies (larger scales) comparing

with the model functions (curves *1* in Figs. 1 and 2). This means that using the models in the form of Eq. (6) for calculations of the optical waves characteristics we can expect the agreement with experiments only for the finite ranges of spatial and temporal scales.

1.2. Optical mesuring the pulsation spectra of the refractive index in the model convection

Analyzing the conclusions of Subsection 1.1, it should be noted that measurements of Ref. 12 were performed in the real atmosphere with both the convective and dynamic components of the turbulence where the latter was caused by the change of the average wind velocity. It is interesting to study the behavior of the spectra of each component individually, since the theoretical estimates of Ref. 14 show that for the atmosphere it is natural to accept the hypothesis that the vertical convective motions do not interact immediately with the small–scale dynamic turbulence caused by the average wind velocity gradient. Although the turbulence of dynamic origin engenders the vertical pulsations as well their contribution to the resultant variance for the developed convection is negligible and we can consider that the vertical motions are caused only by convection. Thus, the atmospheric turbulence can be considered as an additive sum of the convective and dynamic components.

Results of the study of the temperature pulsation spectra in the model convective flow are given here. This regime of a purely temperature turbulence in the absence of wind is realized in the free atmosphere for the unstable stratification.

The turbulence is investigated on the basis of the optical measurements. Assuming uniformity and isotropy of the refractive index fluctuations, the following functional relationship exists[10] between the statistical characteristics of optical waves $B(\rho)$ and the spectrum $\Phi_n(\kappa)$ ($\kappa = |\kappa|$):

$$B(\rho) = \int_0^{+\infty} d\kappa\kappa\, f(\kappa, L)\, \Phi_n(\kappa)J_0(\kappa\rho), \qquad (7)$$

where ρ is the distance between the observation points in the plane perpendicular to the direction of light propagation, $f(\kappa, L)$ is the spectral filtering function defining the range of the spectrum $\Phi_n(\kappa)$ which gives the main contribution to the fluctuations of this wave parameter, $J_0(\kappa, \rho)$ is the Bessel function of the first kind and L is the length of the optical path. It was shown in Ref. 15 that the solution of integral equation (7) for obtaining the spectrum from the measurements of $B(\rho)$ for the finite range of variation of ρ is the correct inverse problem.[16]

The experimental setup used to model the purely temperature convection was the 2×1 (m^2) surface being heated. The heating elements located under the surface allowed us to obtain different temperature gradients: the value of the gradient was determined by a current carried by the heating elements. To reconstruct the form of the function $\Phi_n(\kappa)$ in both inertial and energy ranges of the wave numbers κ, simultaneous measurements of both the intensity and phase fluctuations were needed. The setup used to measure the phase consisted of the dual–beam Michelson interferometer.[15] The baseline ρ (the distance between the beam centers) varied from 1 cm to 0.5 m.

The phase difference between the centers of the spatially—spaced Gaussian beams was measured by the analogue—to—digital phase meter[5] with the threshold sensitivitybeing equal to 0.1 radian. The intensity fluctuations were recorded on the axis of one of the beams. The simultaneous realizations of the random processes of the intensity and phase difference fluctuations were statistically processed.

The time—dependent coefficients of correlation $b_s(\tau)$ and $b_x(\tau)$ for $\tau \le T$ were estimated from the synchronous realizations of the intensity and phase difference fluctuations of finite duration T. The spectrum $\Phi_n(\kappa)$ from Eq. (7) was reconstructed on the basis of the the correlation coefficients $b_x(\tau)$ and $b_s(\tau)$ corresponding to the same realization.

As is well known, the turbulent regime in convection has the property of the similarity, i.e., the values of the viscosity coefficient and thermal diffusivity must be eliminated from the basic parameters. The turbulent characteristics must depend solely on the parameter having the dimensions of length, i.e., on the altitude above the surface being heated. Therefore, investigation of the spectra of the refractive index pulsations in model flow as a function of altitude seems to be interesting. To this end, the intensity and phase difference fluctuations of the radiation propagating in the convective flow along a path of length $L = 2$ m were measured. The altitude of the path above the underlaying surface was changed (8, 14, and 21 cm). The radiation of a He—Ne was splitted into two identical collimated beams whose structure was close to the unbounded planar wave. The beams were spaced in the horizontal direction at the distance ρ. The average v velocity of the buoyancy of the temperature inhomogeneities of air was measured that allowed one to go over from the time variable $\hat{b}_x(\tau)$ to the spatial variable $b_x(\rho) = b_x(v\tau)$. The estimates of the normalized correlation functions for the intensity fluctuations $\hat{b}_x(\tau)$ and for the phase fluctuations $\hat{b}_s(\tau) = [1 - D_s(\rho)/D_s(\rho_m)]$ at different altitudes are shown in Fig. 3. The most typical feature is the increase of the correlation length of the phase fluctuations with h which can be interpreted as the vertical growth of the outer scale of the turbulence L_0 since in free convection the turbulent inhomogeneities grow larger with altitude. The phase correlation was measured at the distance from 1 up to 13 cm that allowed one to reconstruct the spectrum $\Phi_n(\kappa)$ for 0.08 cm$^{-1} \le \kappa \le 1$ cm^{-1}. The intensity correlation was measured at 100 points with the steps $\Delta = 0.026$ cm, corresponding spectral range was 0.4 cm$^{-1} \le \kappa \le 20$ cm^{-1}. Measuring simultaneously the phase and the intensity fluctuations makes it possible to reconstruct the spectrum in both energy and inertial ranges. Joining of the spectra reconstructed from the intensity and phase measurements allowed one to extend the range of reliable reconstruction comparing with the measurements in which either intensity fluctuations or phase fluctuations were measured. The results of calculations showed that with 8% random error in the measurement of the correlation coefficients the spectrum was estimated in the range 0.05 cm$^{-1} \le \kappa \le 20$ cm^{-1} with the error not greater than the measurement error.
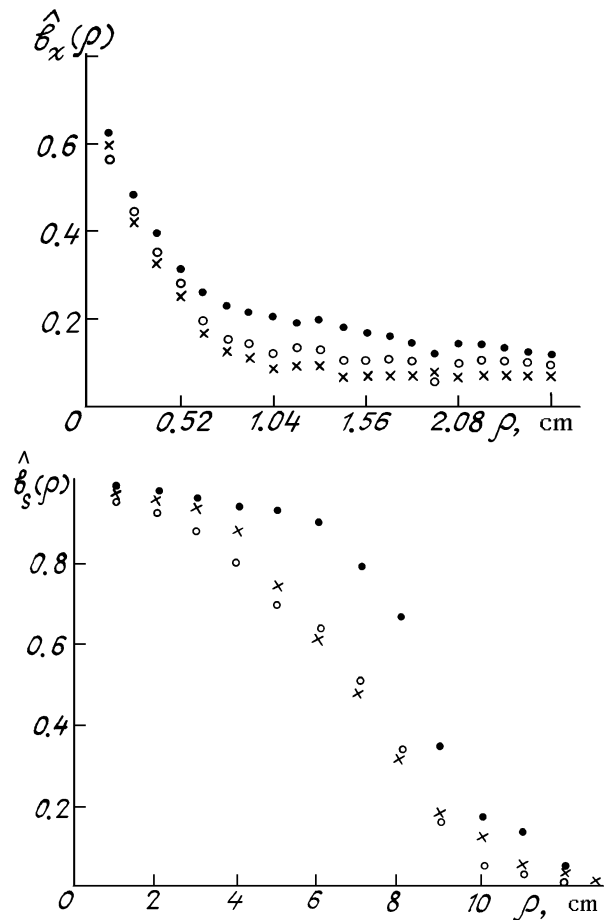

FIG. 3.   *The normalized correlation function for the intensity fluctuations (a) and phase fluctuations (b): crosses correspond to $h = 8$ cm, empty circles correspond to $h = 14$ cm, and filled circles correspond to $h = 21$ cm.*

The pulsation spectra of the refractive index at different altitudes above the underlying surface are shown in Fig. 4. Two regions can be clearly distinguished in the behavior of each spectrum: the region of saturation of the spectrum and the region in which the function $\Phi_n(\kappa)$ is described by the power—law dependence. The slope of the spectrum is close to $11/3$, only for $h = 8$ cm it deviates. The most substantial difference between the spectra with h can be observed in the low—frequency region which is associated with the monotonic growth of the turbulence scale. In addition, the vertical profile $L_0 = L_0(h)$ is closer to the model $L_0 = 2\sqrt{h}$ (cm) given in Ref. 7 than to the model $L_0 = Kh$, where K is the von Karman constant given in Ref. 10. The reconstructed spectra $\Phi_n(\kappa)$ follow the power—law dependence up to $\kappa = 20$ cm^{-1} which leads to the conclusion that the inner scale l_0 of the given turbulent medium is not greater than 2 mm.

1.3. Rconstruction of the turbulence spectrum from the amplitude and phase measurements

The spatial correlation functions for the phase fluctuations used in Subsections 1.1 and 1.2 to reconstruct

the spectrum $\Phi_n(\kappa)$ require sufficiently long–time measurements during which it is impossible to quarantee the stability of the atmospheric characteristics. The aforementioned considerations lead to the idea of reconstruction of the spectrum from the synchronous measurements of the temporal spectra of the intensity and phase difference fluctuations with the constant baseline. This was the reason for collaboration of the Institute of Atmospheric Optics of the Siberian Branch of the Russian Academy of Sciences and the Institute of Atmospheric Physics of the Russian Academy of Sciences.
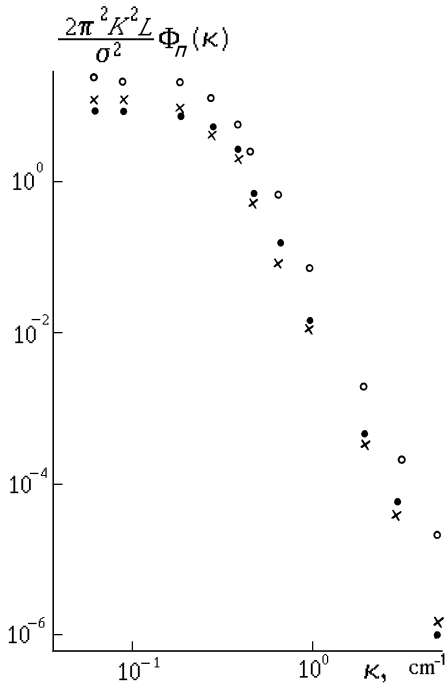

FIG. 4. The reconstructed spectral power density of the fluctuations of the refractive index (at different altitudes, designations are the same as in Fig. 3).

The equation

$$\omega W_x(\omega) = 2.6 C_n^2 k^{7/6} L^{11/6} X \int\limits_X^\infty d\kappa \left(1 - \frac{\sin \kappa^2}{\kappa^2}\right) \times$$
$$\times \left(\kappa^2 - X^2\right)^{-1/2}\kappa^{-8/3}\, \varphi\!\left(\kappa D^{-1/2}\right), \qquad (8)$$

where $X = \omega\sqrt{\frac{L}{k}}/v$ is the dimensionless frequency, L is the optical path length in the atmosphere, k is the wave number of the radiation, v is the wind velocity in the direction transverse to the direction of light propagation, $D = L/k\eta^2$ relates the temporal spectrum of the intensity fluctuations $W_x(\omega)$ with the function φ being the correction for the one–dimensional power–lower spectrum of the refractive index field

$$E_n(\kappa) \simeq 0.4\, C_n^2 k^{5/3}\, \varphi(\kappa\eta), \qquad (9)$$

where C_n^2 is the structure parameter of the refractive index, $\eta = v^{3/4} < \varepsilon >^{-1/4}$ is the Kolmogorov scale, ε is the rate of dissipation of the turbulent energy, and v is the kinematic viscosity of air. The correction $\varphi(\kappa\eta)$ equals to unity in the inertial range, while in the dissipation range it produces the

decay. The problem of the spectrum reconstruction reduces to finding this function.

To study the spectrum $E_n(\kappa)$ in the inertial and energy ranges the phase measurements are preferable.[3,7] The equation

$$\omega W_{\delta s}(\omega) = 10.4 C_n^2 k^{7/6} L^{11/6} \sin^2\!\left(\frac{\rho}{2}\sqrt{\frac{k}{L}}\,X\right) \times$$
$$\times X \int\limits_X^\infty d\kappa \left(1 + \frac{\sin \kappa^2}{\kappa^2}\right)\left(\kappa^2 - X^2\right)^{-1/2}\kappa^{-8/3}\, \varphi\!\left(\kappa D^{-1/2}\right) \quad (10)$$

relates the temporal spectrum of the phase difference fluctuations $W_{\delta s}(\omega)$ at the points separated at the distance ρ in the plane, perpendicular to the direction of wave propagation with function $\varphi(\kappa\eta)$. The spectrum of the phase difference carries a larger amount of information about the spectrum $E_n(\kappa)$ in the region of small wave numbers than $W_x(\omega)$. But now it is difficult to ensure the required accuracy of measurements of the phase differences in the high–frequency range.[5] Therefore, we can use the synchronous measurements of both spectra and the simultaneous solution of Eqs. (8) and (10) for reconstruction of the turbulence spectrum.

To determine the component of the average wind velocity in the direction perpendicular to the path which enter into Eqs. (8) and (10), it is necessary to measure the velocity and direction of wind synchronously with the optical measurements. The independent measurements of the structure constant of the temperature field C_T^2 are also needed since $C_n^2 \approx C_T^2 <\frac{\partial n}{\partial T}>^2$.

The diagram of the experimental configuration is shown in Fig. 5. The measurements were performed over the steppe near Tsymlyansk. The He–Ne laser beams propagated over the even horizontal surface at an altitude of 1.5 m above the ground. The path length was 47 m.
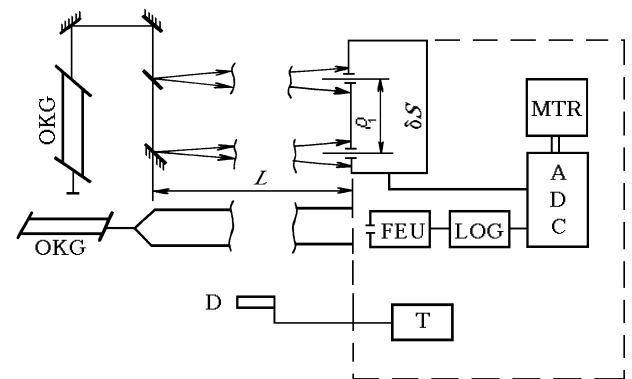

FIG. 5. Diagram showing the experimental configuration. OKG is the He–Ne laser; δS is the optical phase meter; FEU, LOG, and ADC are the components of the scheme (photodetector, amplifier, and analogue–to–digital converter); MTR is the multichannel tape–recorder; and, D and T are the sensor and meter of temperature pulsations.

We used a wide ($\rho_0 = 5$ cm) collimated Gaussian beam for the amplitude measurements. Two identical beams separated at the distance ρ were propagated parallel to the first beam (see Fig. 5). The phase difference fluctuations between the beam centers in the receiving plane were

recorded by means of the optical phase—meter.[5] The measurements of the phase differences were performed with the baselines ρ being equal to 55 and 5 cm. The spectra of the phase difference fluctuations in the centers of the spaced beam for the parameters of our experiment coincided[7] with high accuracy with the spectra of the planar wave. Phase difference and log—amplitude fluctuations were stored using the multichannel tape—recorder with a sampling frequency of 16 kHz.

The average velocity and direction of wind were measured by a cup anemometer and bearing meter mounted at an altitude of 1.5 m above the ground near the center of the optical path. The sensor for measuring the temperature micropulsations was placed here too. Determination of C_T^2 was based on the measurements of the mean square temperature fluctuations at a frequency of ≈ 3 Hz.

To calculate the spectra $W_{\delta s}$, the 24—s records of the phase difference fluctuations were employed, and to calculate the spectra $W_x(\omega)$ — the 8—s records. Three spectra of the intensity fluctuations multiplied the frequency are shown at the top of Fig. 1, and the phase spectra obtained with the baselines 55 and 5 cm corresponding to preceding baselines — at the bottom of the figure. The spread (variance) of the experimental data is shown by the vertical bars. Different sensitivity of $\omega W_x(\omega)$ and $\omega W_{\delta s}$ to the refractive index spectrum at different frequencies is shown from Fig. 6.
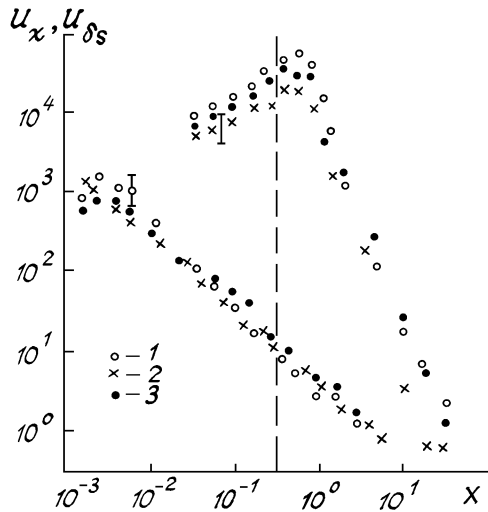

FIG. 6. The dimensionless spectra of the log—intensity fluctuations of the light wave $U_x = \omega W_x/(2.6 C_n^2 k^{7/6} L^{11/6})$ are shown as the upper band of the experimental data. The low band of the experimental data are the dimensionless spectra of the phase difference fluctuations $U_{\delta s} = \omega W_{\delta s}/(1.04 \cdot 10^{-6} C_n^2 k^{7/6} L^{11/6})$; 1 and 2) ρ = 55 cm and 3) ρ = 5 cm.

The idea of solving Eqs. (8) and (10) simultaneously for reconstruction of the turbulence spectrum over the entire frequency range is expressed mathematically in the following form. The sought—after spectrum is found by means of solving the integral equation $f = K\varphi$, in which the compound kernel

$$K(x, y) = \{K_{\delta s}(x, y), \, x \le x_0, \, K_x(x, y), \, x > x_0, \quad (11)$$

is used and the measurable function f is represented in the form

$$f(x) = \{W_{\delta s}, \, x \le x_0, \, W_x, \, x > x_0, \quad (12)$$

so that to provide the continuity of the solution in the joining point x_0. The choice of the joining point is dictated by the compromise between the increasing error φ in the reconstruction based only on Eq. (8) with decrease of the wave number and the reliability of measurements of $W_{\delta s}$ deteriorating in the direction toward the larger wave numbers. The chosen point x_0 is shown in Fig. 6 by the dashed line.

It should be noted that Eqs. (8) and (10) are Abel's integral equations. Their solution with the use of the experimental data is the incorrect inverse problem and requires the regularization.[16,20–22] The method of statistical regularization[20,21] was used to solve Eqs. (8) and (10)

From Eqs. (8) and (10) we can obtain only a certain function $\varphi_1(\kappa)$ $\left(\text{for } \kappa = x\sqrt{\dfrac{k}{L}}\right)$, so far as we do not know the values of η for each spectrum. Independent measurements of the energy dissipation rate ε allow one to go over to the universal function $\varphi(\kappa\eta)$. Let us represent the obtained result in the generally accepted[23] form of Eq. (9) for the one—dimensional spectrum

$$E_1^n = \frac{5}{12} C_n^2 \int\limits_x^\infty d\kappa \kappa^{-8/3} \varphi_1(\kappa) \,. \quad (13)$$

The spectrum $\tilde{E}_1^n = E_1^n / \frac{5}{12} C_n^2$ calculated using the values of $\varphi_1(\kappa)$, is shown in Fig. 7. In the small scale region the spectrum decays steeply, this corresponds to the viscous range. The analogous result was obtained earlier in Ref. 24.
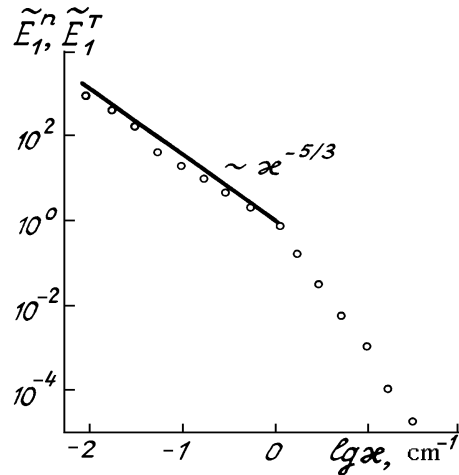

FIG. 7. The one—dimensional spectrum of the refractive index calculated from formula (13) for φ_1 (circles) and one—dimensional spectrum of the temperature from Ref. 26 (solid curve).

As a results of simultaneous measurements, the authors of Ref. 19 succeeded to advance toward the low—frequency range (comparing with Ref. 24) in the measurements of the refractive index spectrum. In this frequency range the temperature spectra were measured with resistance thermometers.[25,26] The fluctuations of the refractive index in the optical range are determined primarily by the temperature fluctuations, therefore we can compare the form

of the spectra of these quantities. The temperature spectrum being a generalization of a series of measurements with negative values of the Richardson number ($R_i = 0,..., -2$) is shown in Fig. 7 by the solid curve.[26] For comparison, this spectrum was re−normalized $\tilde{E}_1^T = E_1^T / C_T^2$ at $z = 1.5$ m.

The proposed procedure of the optical measurements and processing of the results allowed one to reconstruct the refractive index spectrum in the very wide range of scales (from 1.5 mm to 5 m) covering the inertial and viscous ranges.

We will further return to these data and to the reconstruction of the turbulence spectra from the temporal phase measurements once again in Subsection 2.2.

1.4. Measuring the turbulence spectrum from the data on the randomly displaced beams

In Subsection 1.1 we noted the strong dependence[8,9,11] of the spatial correlation function of the random displacement $B_c(x, \rho)$ of the parallel light beams separated at the vector $\rho = \rho(y, z)$ on the behavior of the fluctuation spectrum of the refractive index $\Phi_n(0, \kappa)$ in the energy range of the wave numbers κ. From the results of Ref. 27 it follows that in the case of horizontal paths of propagation the functions $B_c(x, \rho)$ and $\Phi_n(0, \kappa)$ are related by a two−dimensional Fredholm integral equation of the first kind

$$B_c(x, \rho) = \int\int d^2\kappa \, \Phi_n(0, \kappa) \, P(x, \kappa) \exp(-i\,\kappa\rho) . \quad (14)$$

Here

$$P(x, \kappa) = 2\pi x^3 \kappa^2 \int_0^1 d\xi \, (1 - \xi)^2 \exp\left[-\kappa^2 \, a_{\text{eff}}^2 \, (\xi - 1)^2/2\right] ,$$

$$a_{\text{eff}}^2(x) = a^2\left[(1 - x/F)^2 + \Omega^{-2} + 2^{-6/5} \, D_s^{6/5}(2a) \, \Omega^{-2}\right]$$

is the square effective radius of the beam at the distance x; a is the initial radius of the beam, F is the radius of the phase front curvature in the center of the transmitting aperture, $\Omega = ka^2/x$ is the Fresnel number, $k = 2\pi/\lambda$ is the wave number, and $D_s(2a)$ is the phase structure function of spherical wave calculated on the diameter of the transmitting aperture.
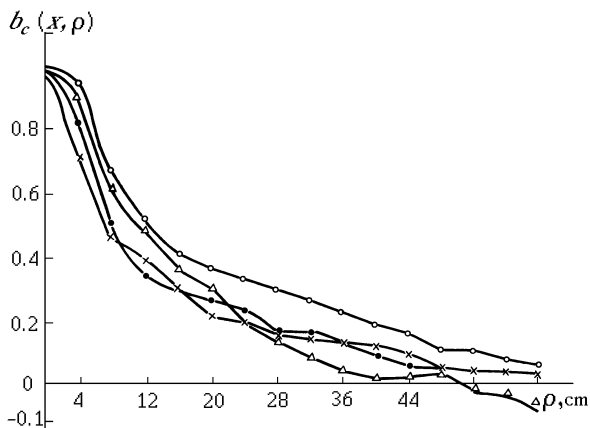

FIG. 8. The experimental spatial correlation coefficient for the random displacements of the parallel focused light beams obtained in Ref. 9. Filled circles correspond to $v = 0.64$ m/s, empty circles correspond to $v = 1.4$ m/s, crosses correspond to $v = 1.8$ m/s, and triangles correspond to $v = 2$ m/s.

Unlike the equations used before, Eq. (14) does not impose the limitation of smallness of the intensity fluctuations and allows one to use the optical beams of the arbitrary shape.

The results of the spectrum reconstruction using Eq. (14) are given here. We used the experimental data of Ref. 9 for calculation of the correlation coefficient of the time−dependent displacements of the light beam $b_c(x, \rho = v\tau)$ (τ is the time delay and v is the wind velocity in the direction transverse to the direction of wave propagation). The coefficient of the spatial correlation of the displacement $b_c(x, \rho) = B_c(x, \rho = v\tau)/B_c(x, 0)$ plotted from the experimental data given in Ref. 9 for different values of the wind velocity v ($v = |\mathbf{v}|$) is shown in Fig. 8.

In what follows we will use normalized Eq. (14) involving the correlation coefficient

$$b_c(x, \rho) = \int\int d^2\kappa \, U(x, \kappa) \, P(x, \kappa) \exp(-i\,\kappa\rho) \quad , \quad (15)$$

where

$$U(x, \kappa) = \frac{\Phi_n(0, \mathbf{k})}{\int\int d^2k \, P(x, \mathbf{k}) \, \Phi_n(0, \mathbf{k})} \quad (16)$$

in the left side.

Thus using the data of measurements of $b_c(x, \rho)$ for the inverse Fourier transform in Eq. (15) (or the Fourier−Bessel transform for the isotropic spectrum) we can determine the normalized spectrum $U(x, \kappa)$.

Let us assume that the fluctuation spectrum of the refractive index is isotropic. In this case, solving Eq. (15) by the Tikhonov method,[28,29] we obtain the estimate of the normalized spectrum in the form of Eq. (16)

$$\hat{U}(x, \kappa) = \frac{1}{2\pi \, P(x, \mathbf{k})} \int_x^\infty d\rho\rho \, J_0(\kappa\rho) \, b_c(x, \rho)\left[1 + \frac{\alpha\rho^2}{4\pi^2}\right]^{-1} . (17)$$

In relation (17) we used the data on $b_c(x, \rho)$ shown in Fig. 8. Integral in Eq. (17) was numerically calculated. The function $P(x, \kappa)$ was calculated taking into account the parameters of the optical experiment described in Ref. 9. The regularization parameter α was chosen[28,29] starting from the spread of the initial data on the correlation coefficient.[9]

So far as the correlation coefficient $b_c(x, \rho)$ was measured for the separation of the observation points $\rho \le 0.6$ m with the step being equal to 0.06 m (see Ref. 9), the spectrum $\hat{U}(x, \kappa)$ can be reconstructed for the wave numbers $\kappa \in [1.6 \text{ m}^{-1}, 20 \text{ m}^{-1}]$.

The reconstructed spectrum $\hat{U}(x, \kappa)$ is shown in Fig. 9. The straight line corresponds to the power−law dependence $\kappa^{-11/3}$ characterizing the inertial range of the spectrum; in the region of small wave numbers the spectral density deviates from the power−law dependence. A certain "trend" to saturation on the constant level takes place. It was found that the deviations of the spectrum $\hat{U}(x, \kappa)$ in the experiment attendant to changes in the average wind velocity v lie within the limits of the reconstruction errors. Therefore, it is impossible to determine the dependence of $\hat{U}(x, \kappa)$ on the wind velocity.
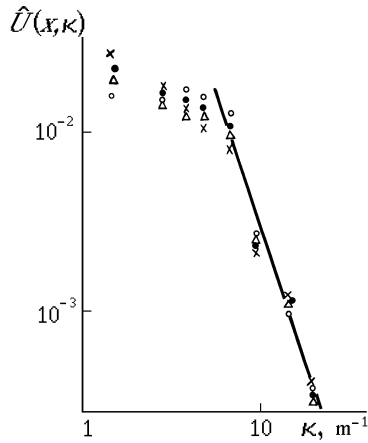
FIG. 9. The normalized spectrum $U(x, \chi)$ reconstructed from the experimental data given in Ref. 9. Designations are the same as in Fig. 8.

In conclusion we note that the results of reconstruction of the atmospheric turbulence spectrum agree with the results obtained on the basis of the phase measurements.[12,19]

2. ANALYSIS OF THE MODELS FOR THE LOW–FREQUENCY SPECTRUM OF THE ATMOSPHERIC TURBULENCE

It is well known that the atmospheric turbulence as any motion with dissipation, can exist as the stationary phenomenon only in the presence of energy sources. Energy enters into the turbulent motion from the larger scales of motion. This can be the convective flows due to heating of the Earth, change of the average wind, and gravitational waves. These sources transfer the energy to the turbulence primarily through the energy range in which the main portion of the energy of turbulence is concentrated. As a rule, the Reynolds numbers of the initial flow are large that leads to loss of its stability and formation of the vortexes whose dimensions are of the order of the initial flow having the sense of the outer scale of the turbulent motion L_0. The turbulent energy is consumed in the dissipation range in which the energy is transformed into the heat due to viscosity. If the Reynolds number of the initial flow is sufficiently large, the dissipation range is separated from the energy range by the region of the wave numbers κ satisfying the condition

$$L_0^{-1} \ll \kappa \ll l_0^{-1} , \tag{18}$$

where l_0 is the inner scale of the turbulence called the inertial range. The behavior of the atmospheric turbulence in the region defined by inequality (18) is entirely determined by the rate of dissipation of the turbulent energy ε and by a certain external parameter N characterizing the sources. The consequence of this for the locally uniform and isotropic turbulence is the two–thirds law of the Kolmogorov––Obukhov, which corresponds in the spectral language to the five–thirds law

$$E(\kappa) = C\varepsilon^{2/3} \kappa^{-5/3} , \tag{19}$$

where $E(\kappa)$ is the one–dimensional spectral power density of the kinetic energy and C is the constant of the order of unity.[23] The spectrum $E(\kappa)$ or the spectrum of the pulsation refractive index $\Phi_n(\kappa)$ corresponding to it does not allow

one to calculate the statistical characteristics of the phase fluctuations of optical waves propagating through the turbulent atmosphere so far as the latter is determined by the behavior of the turbulent energy spectrum in the energy range. At the same time, a number of the experimental results, i.e., measurements of the correlation and structure functions of the phase fluctuations of optical waves,[12] and the correlation of the displacement of the centers of gravity of the spatially bounded Gaussian beams[9] as well as the direct measurements of the structure function of the temperature fluctuations[6] show the substantial deviation of the real spectra $E(\kappa)$ (and of the corresponding spectra $\Phi_n(\kappa)$) from the model spectra described by Eq. (19) in the region of small κ. The attempts to measure the spectra of temperature pulsations by indirect methods, using the measurements of the fluctuations of optical waves propagating in the atmosphere, were undertaken in Ref. 12. These measurements, in particular, showed that the reconstructed pulsation spectra of the refractive index are fairly described by the von Karman model taking into account the finiteness of the outer scale of the turbulence.[30]

2.1. The most widely used models of the turbulence spectra in the low–frequency range

Unlike the inertial range of the wave numbers κ, the spectral power density of the fluctuations of the refractive index $\Phi_n(\kappa)$ in the energy range (i.e., for $\kappa \lesssim L_0^{-1}$) is no longer the universal function.[30] It is well known that the spectrum in the low–frequency range depends on both the topography of the underlaying surface (at low altitudes) and the meteorological conditions. Naturally, the shape of the spectrum will change, for example, with the change of the altitude above the underlying surface as well as with the change of the degree of the thermodynamic stability of the turbulence. Therefore, an assumption about local uniformity and isotropy of the turbulence is no longer valid.

At the same time sufficiently simple and convenient models of the spectrum are needed for the calculation of the statistical characteristics of optical waves (estimates of variance of fluctuations).

At present most applicable are the following isotropic models of $\Phi_n(\kappa)$ taking into account the deviations from the power–law dependence in the region of the outer scale of the turbulence:

— the von Karman model[30,6]

$$\Phi_n(\kappa) = 0.033 \, C_n^2 \left(\kappa^2 + \kappa_{01}^2\right)^{-11/6} , \tag{20}$$

— the exponential model[35,11]

$$\Phi_n(\kappa) = 0.033 \, C_n^2 \, \kappa^{-11/3} \left\{1 - \exp[-\kappa^2/\kappa_{02}^2]\right\} , \tag{21}$$

— the Greenwood–Tarazano model[33]

$$\Phi_n(\kappa) = 0.033 \, C_n^2 L_{03}^{11/6} \left(\kappa^2 L_{03}^2 + \kappa \, L_{03}\right)^{-11/6} . \tag{22}$$

Here $\kappa_{01} = 2\pi/L_{01}$, $\kappa_{02} = 2\pi/L_{02}$, and L_{01}, L_{02}, and L_{03} are the corresponding outer scales for the models described by Eqs. (20), (21), and (22). Naturally, these models describe but approximately the behavior of the spectrum in the low–frequency range. The main feature of all these models is the fact that $\int_0^\infty d\kappa\kappa\Phi_n(\kappa)$ is finite, consequently, any finite

volume has the finite energy of the turbulence. These models adequately describe the inertial range of the spectrum

$$\Phi_n(\kappa) \sim 0.033 C_n^2 \kappa^{-11/3} \text{ for } \kappa \gg L_0^{-1} .$$

The parameters of the models described by Eqs. (20), (21), and (22), such as C_n^2 and L_0 can, in their turn, be described by the independent models describing the variation in the parameters, for example, as a function of the altitude h.

The models describing the behavior of C_n^2 are more applicable. In this case the input parameters of the resultant model are:

    — the characteristic near–ground value of C_n^2 for the given place and its possible variations (diurnal variations and seasonal trends),

    — the vertical profile of $C_n^2(h)$, and

    — the variations of the integral value $\int\limits_0^\infty dh \, C_n^2(h).$

The information about the outer scale of the turbulence is too limited, since the existence itself of this outer scale has been yet discussed up to date. At low altitudes above the underlying surface h for the convective turbulence the generally accepted model[41] is $L_0 \sim h$. Several authors recommend the model $L_0 \approx 2\sqrt{h}$ (here h and L_0 are measured in meters) for the altitudes $h > 20$ m. The value $L_0 = \text{const}$ is generally accepted for the altitude above 100 m.

At the same time the measurements of $L_0(h)$ which are described by the analytical formula

$$L_0(h) = \frac{4}{1 + \left(\dfrac{h - 8500}{2000}\right)^2} , \tag{23}$$

are well known[31] in France (Observatory de Haute Provence, France) as well as in Chile[34] (ESO, La Silla, Chile), where

$$L_0(h) = \frac{5}{1 + \left(\dfrac{h - 7500}{2000}\right)^2} , \tag{24}$$

which are sufficiently close in values. I am aware of the fact that the outer scale in models described by Eqs. (20), (21), and (22) and the outer scale L_0 in Ref. 34 introduced by V.I. Tatarskii (see Ref. 10) are somewhat different but, undoubtedly, they are comparable.

2.2. Intercomparison of the models for the turbulence spectra and the data of the optical measurements

In my opinion, it is most objective to discuss some measurable optical parameters rather than to compare the models.

Comparison of three models of $\Phi_n(\kappa)$ described by Eqs. (20) and (21) and by the Kolmogorov–Obukhov model is shown in Fig. 1 using the measurements published in Ref. 19. Let us compare the obtained experimental data with the results of calculations of the normalized phase structure function corresponding to the isotropic models of the spectrum. The correlation coefficients $b_s(y)$ for Eqs. (20) and (21) are represented in the following way:

$$b_s(y) = \frac{\Gamma(1/6)}{\pi} \left(y\kappa_{01}/2\right)^{5/6} K_{-5/6}\left(y\kappa_{01}\right) , \tag{25}$$

$$b_s(y) = {}_1F_1\left(-\frac{5}{6}, 1; (\kappa_{02}y/2)^2\right) - (y\kappa_{02}/2)^{5/3}/\Gamma\left(\frac{11}{6}\right), \tag{26}$$

where $K_{-5/6}(x)$ is the McDonald function and ${}_1F_1(\alpha, \beta; x)$ is the degenerate hypergeometric function. Comparing the calculated and experimental correlation coefficients (Fig. 1) we choose the parameters κ_{01} and κ_{02} according to the criterion of the best agreement of $D_s(y)/D_s(y_m)$ with the quantity $[1 - b_s(y)]$ in the saturation region (curves 1 and 3) and in the region of power–law increase ($D_s(y) \sim y^{5/3}$) (curves 2 and 4). It can be seen from this comparison that models (20) and (21) fairly describe as a whole the trend in the behavior of the phase structure function. However, they cannot ensure the agreement in the entire range of the observation points. For model (20) the values of the outer scale L_0 ensuring the best agreement (in Fig. 1) lay in the range 0.96–1.96 m. This value of the outer scale are comparable with the altitude above the underlying surface at which the measurements were performed[19] ($h = 1.2–1.5$ m).

3. INVESTIGATION OF THE ANISOTROPY OF THE ATMOSPHERIC TURBULENCE SPECTRUM IN THE LOW–FREQUENCY RANGE

One of the most important properties of the atmospheric turbulence is continuity, that is, the contribution to the pulsations of the refractive index at each moment comes from the inhomogeneities of all scales. The largest inhomogeneities are the inhomogeneities associated with the breakdown of the average large–scale motions: zone winds, atmospheric fronts, and nonuniformities of the radiation regime. All these motions breaking down due to the instability serve as a basis for the entire spectrum of the turbulent inhomogeneities. The region of the large–scale inhomogeneities is most closely related with all local meteorological parameters, first of all, with the fields of the wind velocity and temperature and their gradients. In the surface layer this region (in which the dimensions of the inhomogeneities exceeds several meters) is called the range of the energy–producing vortex has, as a rule, anisotropic properties, i.e., these inhomogeneities have the properties depending on the direction.

Naturally, the properties of the corresponding statistical characteristics of optical waves are also dependent on the direction.

Let us consider the pecularities of the random displacements of the image formed in the surface layer of the atmosphere on the horizontal atmospheric path. It is well known that when the image is formed the phase fluctuations are very important. Therefore, if the atmospheric turbulence spectrum is anisotropic, the anisotropy of jitter in the low–frequency range could be expected.

The position of the image in the focal plane of the lens with radius R and focal length F is determined by the position of its center of gravity[36,37]

$$\rho_c = \int\int d^2\rho \rho I_F(\rho) \bigg/ \int\int d^2\rho \, I_F(\rho) , \tag{27}$$

where $I_F(\rho)$ is the intensity distribution in the focal plane of the lens which is given by the formula

$$I_F(\rho) = \frac{k^2}{4\pi^2 F^2} \int\int d^2\rho_1 d^2\rho_2 U(\rho_1) U^*(\rho_2) \exp\left[-i\frac{k\rho}{F}(\rho_1 - \rho_2)\right],$$

(28)

where $U(\rho)$ is the field propagated through the turbulent layer. The integration is performed over the illuminated surface of the lens in integral (28). So far as the main contribution to the jitter in the image comes from the phase fluctuations neglecting the amplitude fluctuations we obtain the following equation:

$$\langle\rho_c^2\rangle = \frac{F^2}{k^2\Sigma^2} \int\int_R d^4\rho_{1,2} \nabla^2 B_s(\rho_1, \rho_1)$$

(29)

for the variance of the displacement of the center of gravity. Here Σ is the area of the illuminated surface of the lens, $B_s(\rho_1, \rho_2)$ is the correlation function for the phase fluctuations of optical wave $U(\rho)$.

As a consequence of Eq. (29), we can write down the corresponding equation for the jitter components (ρ_z, ρ_y) of the vector ρ_c. The estimate of the variances $\langle\rho_c^2\rangle = \langle\rho_y^2\rangle + \langle\rho_z^2\rangle$, $\langle\rho_y^2\rangle$, and $\langle\rho_z^2\rangle$ can be obtained with the use of Eq. (29) with the known correlation (or structure) function for the phase fluctuations.

To investigate the variance of the jitter in the image in two perpendicular directions[37] $\langle\rho_y^2\rangle$ and $\langle\rho_z^2\rangle$ the follow—up system was developed on the basis of the coordinate—sensitive photodetector allowing one to measure simultaneously the variance of the image jitter. Experiments were performed under conditions of the model thermal turbulence[37] and in the real atmosphere[38] on the uniformly near—ground paths.

Let us first of all consider the results of the model experiment performed in Ref. 37. The setup producing the developed convective turbulence on the 2-m path was used.[39,40] The collimated beam 6 mm in diameter was focused with the objective ($F_2 = 40$ cm) onto the input window of the photodetector. The variances $\langle\rho_y^2\rangle$ and $\langle\rho_z^2\rangle$ were estimated from the 100 s measurements.

The vertical profile of the convective turbulence structure was investigated: the optical beam was propagated at different altitudes above the surface of the thermal turbulence generator. During the experiment the turbulence regime (average gradients of the temperature) remained unchanged. The sharp, especially at low altitudes, difference of the root—mean—square values of the random displacement of the beam in the vertical $\langle\rho_z^2\rangle$ (curve *1*) and transverse $\langle\rho_y^2\rangle$ (curve *2*) directions was observed (see Fig. 10) that indicated on the turbulence anisotropy. Elongation of the largest—scale inhomogenuities of the refractive index, apparently, was maximum at low altitudes, therefore the anisotropy of the properties of the medium was mostly pronounced here. With increase of the altitude the inhomogenuities became more isotropic while the variances $\langle\rho_y^2\rangle$ and $\langle\rho_z^2\rangle$ became comparable. The variances $\langle\rho_y^2\rangle$ and $\langle\rho_z^2\rangle$ were measured at the fixed altitude for different turbulent regimes. At low altitudes the difference between the corresponding variances increased with increase of the temperature gradient (with growth of the thermodynamic instability) which led to the higher degree of anisotropy.

Analogous measurements on the real atmospheric paths were performed in Tsimlyansk and Tomsk. The measurements were performed at the scientific station of the Institute of Atmospheric Physics of the Russian Academy of Sciences

(Tsimlyansk) in August—September, 1978. The gradients of the temperature T, the wind velocity v, and the fluctuations of the jitter in the image of the collimated optical beam on the 40.4 m path (the path of the laser beam propagation was located at an altitude of 1.15 m above the underlying surface) were measured sychronously along with the wind velocity in the local volume measured with the help of the laser Doppler anemometer.
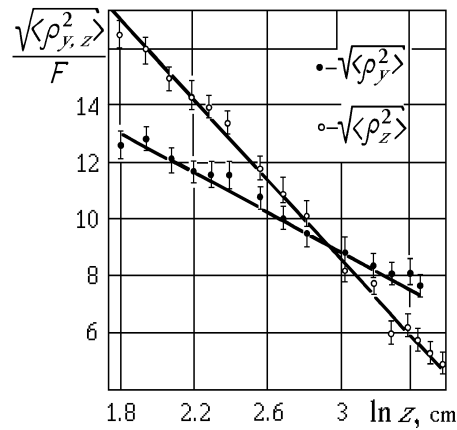

FIG. 10. The vertical profile of the standard deviation of the random displacement of the beam center.

As a result of processing of the measurements of the optical and meteorological parameters, we obtained C_T^2 and C_n^2 from the meteorological measurements, the parameter of the thermodynamic stability B (see Subsection 4.1), variances of the jitter in the image $\langle\rho_y^2\rangle$ and $\langle\rho_z^2\rangle$, and the frequency spectra of fluctuations W_y and W_z as well as the wind velocity components v_y and v_z. The ratio of variances $\langle\rho_z^2\rangle/\langle\rho_y^2\rangle$ characterizes qualitatively the degree of anisotropy of the turbulence. From the measurements of the position of the maximum in the spectra $fW_y(f)$ and $fW_z(f)$, knowing v_y and v_z, we can estimate the outer scale of the turbulence L_0 as well as its components L_{0y} and L_{0z}. In this case L_{0y} and L_{0z} mean the dimensions of the outer scale along two directions.

The ratio of the variances $\langle\rho_z^2\rangle/\langle\rho_y^2\rangle$ characterizing the anisotropy of the turbulence spectrum in the low—frequency range varied from the value of the order of 1 to 2.1. And as early as in these first measurements (1978) it was found that the value L_0 by itself and its components L_{0y} and L_{0z} vary as functions of the value and sign of the parameter of the thermodynamic stability of the atmosphere B. The outer scales of the turbulence L_0 were calculated from the optical measurements and it was found that they lay in the range from 80 cm to 2.5 m (we note that the optical path during these measurements was located at an altitude of 1.15 m). The meteorological measurements including the synchronous measurements of C_T^2 and $(\Delta T/\Delta Z)$, allow one to calculate[10] the outer scale of turbulence L_{0met}:

$$L_{0met} = \left(\frac{C_T^2}{2.8\left(\frac{\Delta T}{\Delta z}\right)^2}\right)^{3/4}.$$

(30)

Comparison of the data of optical measurements of L_0 with $L_{0\text{met}}$ from formula (30) gives the high correlation, although it is impossible to speak about the agreement of the values L_0 and $L_{0\text{met}}$. Note that the outer scale components L_{0y} and L_{0z} were calculated from the measurements of the position of the maximum in the frequency spectra $fW_y(f)$ and $fW_z(f)$ on the basis of the trivial dependence[37,42]

$$f_{\max} = \frac{\sqrt{3}\ \nu_{y,\,z}}{L_{0y,\,z}}\ ,$$

where $f_{\max}$ characterizes the position of maximum in the spectra fW_y and fW_z, ν_y and ν_z are the components of the transverse wind velocity measured in the experiment with the help of the laser Doppler anemometer, L_{0y} and L_{0z} are the components of the outer scale of the turbulence, and $L_0^2 = L_{0y}^2 + L_{0z}^2$.

The variances of the random jitter in the image of the optical source in two perpendicular directions $\langle \rho_y^2 \rangle$ and $\langle \rho_z^2 \rangle$ were measured on the horizontal path of length $L = 1685$ m near stanitsa Zelenchukskaya in 1981. The optical measurements were accompanied by the measurements of the meteorological parameters (T, ν). The jitter in the image was measured in the focus of the telescope comprising the mirror 600 mm in diameter. The ratio of the variances $K = \langle \rho_z^2 \rangle / \langle \rho_y^2 \rangle$ was analyzed.

It was found that for small temperature gradients the value of K averaged over a number of realizations was 1.20, i.e., the vertical random displacements practically coincide with the horizontal displacements. For large gradients of the temperature and low wind velocity the anisotropy becomes more pronounced: $K = 2.89$. With increase of the wind velocity the coefficient of anisotropy ($K = 2.14$) decreases. On the whole, the conclusion is: the anisotropy of the jitter in the image practically always takes place in the surface atmospheric layer (at $h \approx 1.5$–3 m) (see Ref. 38). Mediately, it allows us to speak about the anisotropy of the turbulence.

4. DETERMINATION OF THE RELATIONSHIP OF THE OUTER SCALE OF THE TURBULENCE WITH CHANGE IN THE METEOROLOGICAL SITUATION

We have already noted that the discovered anisotropy of the fluctuations of the position of the center of the optical beam propagated through the turbulent layer of the medium depends on the changing meteorological conditions.

4.1. Relationship of the outer scale of the turbulence with parameter of the thermodynamic stability

It has been established very thoroughly that the behavior of the turbulence spectrum in the low–frequency range for the surface layer is no longer described with the help of the single parameter − the turbulent intensity. It has been also established that the assumption about the local isotropy is incorrect for the real atmosphere and for the large–scale inhomogeneities whose dimensions are close to the outer scale of the turbulence.

Nevertheless, various models describing the spectrum in the region of the large scales in practice are applicable for the calculation of the optical field fluctuations. These models have two parameters. The so–called outer scale L_0 is

used as the second parameter. Various models of the turbulence spectrum were used in calculations, while the agreement between the experimental data and the calculated results was obtained by means of adjusting the parameter L_0. The results obtained in Refs. 18 and 19 showed that the outer scale of the turbulence is comparable with the altitude of the optical beam propagation path above the underlying surface. However, the values of L_0 obtained by various authors were substantially different.

The reason of this difference seems to be the following. The real atmosphere alongside with the small–scale turbulence contains the large–scale motions of different origin. These motions can be caused by the radiative mottled underlying surface, screening of the underlying surface by clouds, and a number of other factors. These large–scale formations can be considered in the surface layer as slow changes of the external conditions determining the production of the small–scale turbulence. In addition, the parameters of the turbulence (and its models) in the surface layer must vary in time with the characteristic scale of these large–scale structures.

Therefore, if we adjust the parameter L_0 of the model, for example, on the basis of the synchronous measurements of the phase fluctuations of the optical wave and the turbulent intensity C_T^2, then these measurements must be accompanied by measurements of the average meteorological parameters. The experimental measurements of optical beams were performed above the uniform underlying surface on the horizontal paths 15, 40, and 45 m in length located at an altitude of 1.2 m above the underlying surface. The phase structure function in Ref. 42 was measured for the separation of the optical beams at the distance $\rho \approx 3$ m, i.e., for the separations at which $D_s(\rho) \approx 2\sigma_s^2$, where σ_s^2 is the variance of the phase fluctuations in the unbounded plane wave.

To perform comparison with the data of Ref. 42, we calculated the variance of the phase fluctuation by the method of smooth perturbation based on the von Karman model of the turbulence spectrum given by Eq. (20) and model (22). It was found that the outer scales L_0 for these models were comparable. The histogram of the measured values of L_0 characterizing the frequency of occurance of a certain value of the outer scale for model (20) is shown in Fig. 11. Histogram of the outer scale distribution for model (22) is shown in Fig. 12. It can be seen from the comparison of these two histograms that the dimension of the outer scale for the Greenwood–Tarazano model is less than that for the von Karman model. So far as the measurements of the scales L_0 shown in Figs. 10 and 11 were performed for changing meteorological conditions, we tried to classify the measurement data in accordance with the thermodynamic instability. The meteorological measurements were used for calculation of the following characteristic:

$$\text{B} = \frac{gh}{\overline{T}}\frac{\Delta T}{\overline{\nu}^2}\ ,\quad \Delta T = \overline{T}_2 - \overline{T}_{0.5}$$

is the temperature difference between the altitudes of 2 and 0.5 m above the underlying surface, $\overline{T}$ and $\overline{\nu}$ are the average temperature and wind velocity at the altitude h, and g is the acceleration due to gravity. This characteristics allow one to classify the data shown in Fig. 10 from the viewpoint of the thermodynamic stability. It was found that the values L_0 greater than the average value shown by Fig. 10 were realized for neutral stratification $B = 0$. For the unstable ($B < -0.01$) and stable ($B > +0.003$)

stratifications the values of L_0 less than the average value were realized, which is quite explicable. Thus, the high level of instability, i.e., the large negative values of the parameter B, correspond to the higher degree of breaking of the initial flow, therefore the probability of occurence of large L_0 is sufficiently small. For high degree of stability (large positive values of B) the initial flow is weakly turbulized, therefore there are deficits of the inhomogeneities of all scales including the inhomogeneities with dimensions of the order of L_0. Finally, the high value of probability of occurence of the large scales is realized for B close to zero (for neutral stratification).
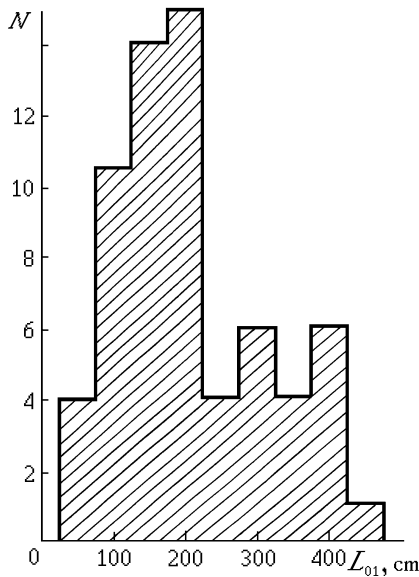

FIG. 11. The histogram of the measured values of the outer scale for turbulence model (20).
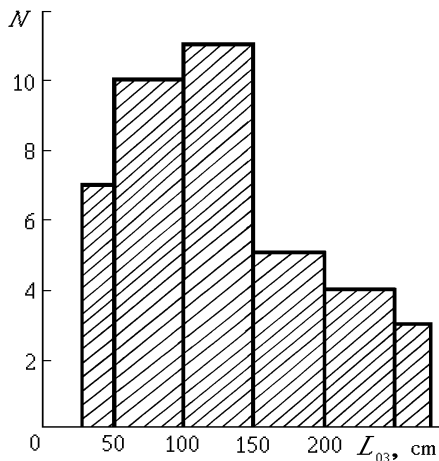

FIG. 12. The histogram of the measured values of the outer scales for turbulence model (22).

At the same time, if one classifies the measured values of L_0 on the basis of the measured average wind velocity, it appears that the lower wind velocity corresponds to the larger values of L_0 and *vice versa*. This confirms the conclusion that the dynamic component of the turbulence is characterized by the smaller–scale structure than the convective component.

4.2. Measurements of the outer scale of the turbulence in precipitations

All measurements described in this paper were performed for the clear atmosphere. In this case, naturally, we considered the regimes of both the convective and dynamic turbulence. However, in practice the clear atmosphere is far from being always encountered. In this connection we turn your attention on the fact discovered by us[35] that the outer scale changes in precipitations in the form of mist.

The measurements of the phase structure function $D_s(\rho)$ of the optical wave propagated through the atmosphere was performed in real time just before and during precipitations.[35] Results of comparison of two runs of measurements of $D_s(\rho)$ for identical values of C_n^2 are shown in Fig. 13. This is confirmed by the agreement of data (straight line) in the region of the power–lower increase of $D_s(\rho)$ shown in Fig. 13. However, in the region of saturation of $D_s(\rho)$, the measurement data are substantially different.
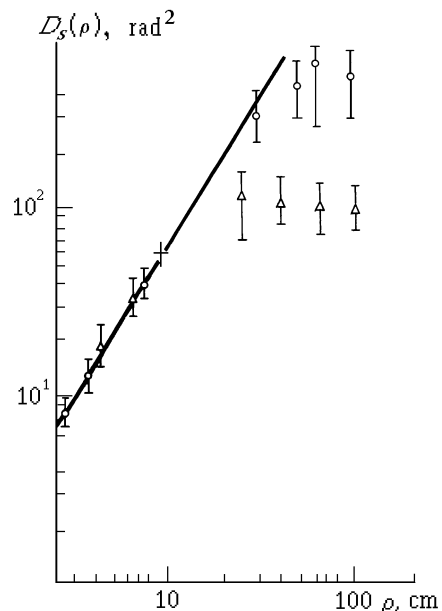

FIG. 13. The phase structure function in the turbid atmosphere (circles correspond to measurements in the clear atmosphere, and triangles correspond to measurements in the turbid atmosphere). Vertical bars show the spread of the experimental data.

It appears that for the clear atmosphere the larger scales of turbulence are developed than those for the turbid atmosphere. The following explanation of this fact is possible: at the moment in which precipitations start, until the turbulent regime remains unchanged, the ordered motion of precipitations in the form of mist breaks the large turbulent structures into smaller parts.

CONCLUSION

Thus, the numerious optical measurements performed in different regions of the CIS showed that in the surface layer of the atmosphere the turbulence spectrum deviates from the Kolmogorov–Obukhov law in the region of scales comparable with the altitudes above the underlying surface.

It was found that the isotropic models of the turbulence spectrum used for description of the phase characteristics have a limited application.

The low–frequency range of the turbulent fluctuations is sharply anisotropic. It was found that the absolute value of the outer scale and its components in two orthogonal directions depend on the class of the instability of the atmosphere. In addition, the presence of the coarse fraction of aerosol in the atmosphere, namely, rain and fog, decreases the effective dimensions of the large–scale turbulence.

The author is aware of the fact that the above–described regularities of the low–frequency region of the turbulence spectrum are applicable in the surface layer of the atmosphere alone. Considerable attention must be devoted to further study of the vertical profile of the outer scale. To this end the astronomic measurements of the jitter in the image of the stars, apparently, will be most useful. These measurements have been already performed. It is necessary only to analyze them. However this will be the subject of our next article.

In conclusion I would like to acknowledge my colleagues Dr. V.V. Pokasov, scientific workers O.N. Emaleev and S.F. Potanin, Dr. V.M. Sazanovich, and Dr. N.S. Tieme for many years of collaboration during which all the experiments were performed.

REFERENCES

1. A.S. Monin and A.M. Yaglom, *Statistical Fluid Mechanics,* (Nauka, Moscow, 1966), Vol. 1, 460 pp.

2. A.M. Obukhov, Izv. Akad. Nauk SSSR, Ser. Geofiz., No. 2, 155–165 (1953).

3. A.S. Gurvich, Izv. Akad. Nauk SSSR, Ser. FAO **4**, No. 2, 160–169 (1968).

4. N.S. Tieme, Izv. Akad. Nauk SSSR, Ser. FAO **8**, No. 1, 90–92 (1972).

5. O.N. Emaleev et al., *"The tracing digital phase meter in the optical range"*, Inventor's Certificate No. 397852, Bull. No. 37, November 17, 1973.

6. G.M. Bouricius and S.F.Clifford, J. Opt. Soc. Am. **60**, No. 11, 1484–1489 (1970).

7. V.P. Lukin and V.V. Pokasov, Izv. Vyssh. Uchebn. Zaved., Ser. Radiofiz. **16**, No. 11, 1726–1729 (1973).

8. M.A. Kalistratova and Vl.V. Pokasov, Izv. Vyssh. Uchebn. Zaved., Ser. Radiofiz. **15**, No. 2, 723–731 (1972).

9. E.I. Gel'fer, A.I. Kon, and A.N. Cheremukhin, Izv. Vyssh. Uchebn. Zaved., Ser. Radiofiz. **16**, No. 2, 245–249 (1973).

10. V.I. Tatarskii, *Wave Propagation in a Turbulent Medium* (McGraw–Hill, New York, 1961).

11. A.I. Kon. Izv. Vyssh. Uchebn. Zaved. Radiofiz. **15**, No. 5, 533–539 (1972).

12. V.P. Lukin et al., Izv. Vyssh. Uchebn. Zaved., Ser. FAO **12**, No. 5, 550–553 (1976).

13. G.M. Jenkins and D.G. Watts, *Spectral Analysis and its Applications* (Holden Day, San Francisko, 1968).

14. S.S. Zilitinkevich, Izv. Akad. Nauk SSSR, Ser. FAO **7**, No. 12, 1201–1209 (1971).

15. V.P. Lukin and V.V. Pokasov, Isv. Vyssh. Uchebn. Zaved., Ser. Radiofiz. **16**, No. 11, 1726–1729 (1973).

16. V.F. Turchin, V.P. Kozlov, and M.S. Malkevich, Usp. Fiz. Nauk **102**, No. 3, 345–386 (1970).

17. D.L. Frid, Proc. IEEE **55**, No. 1, 19–26 (1967).

18. O.N. Emaleev, V.P. Lukin, et al., Izv. Vyssh. Uchebn. Zaved., Ser. Fiz., No. 9, 100–105 (1976).

19. V.P. Lukin, V.V. Pokasov, et al., Izv. Akad. Nauk SSSR, Ser. FAO **13**, No. 1, 90–94 (1977).

20. V.F. Turchin and V.Z. Nozik, Isv. Akad. Nauk SSSR, Ser. FAO **5**, No. 1, 29–38 (1969).

21. V.F. Turchin and L.S. Turovtseva, Opt. Spektrosk. **36**, No. 2, 280–287 (1974).

22. N.S. Tieme and L.S. Turovtseva, *"About the estimate of the spectra of light intensity fluctuations in reconstruction of the tempereture pulsation spectra from the optical measurements,"* Preprint No. 89, Institute of Applied Mathematics, Moscow (1973).

23. A.S. Monin and A.M. Yaglom, Statistic *Fluid Mechanics,* (Nauka, Moscow, 1967), Vol. 2, 453 pp.

24. A.S. Gurvich, N.S. Tieme, et al., Izv. Akad. Nauk SSSR, Ser. FAO **10**, No. 5, 484–492 (1974).

25. S.L. Zubkovskii and B.M. Koprov, Izv. Akad. Nauk SSSR, Ser. FAO **5**, No. 4, 323–331 (1969).

26. J.C. Kaimal and J.C. Wyngaard, Quart. J. Roy. Meteor. Soc. **98**, No. 414, 563–569 (1972).

27. A.I. Kon, V.L. Mironov, and V.V. Nosov, Izv. Vyssh. Uchebn. Zaved., Ser. Radiofiz. **17**, No. 10, 1501 (1974).

28. L.N. Tikhonov, Dokl. Akad. Nauk SSSR **153**, No. 1, 9 (1963).

29. L.N. Tikhonov, Dokl. Akad. Nauk SSSR **163**, No. 1, 6 (1965).

30. J.W. Strohbehn, J. Geoph. Res. **75**, No. 6, (1970).

31. C.E. Coulman, J. Vernin, et al., Appl. Opt. **27**, No. 1, 155–160 (1988).

32. M.M. Colavita, M. Shao, and D.H. Staenin, Appl. Opt. **26**, No. 12, 4106–4112 (1987).

33. D.P. Greenwood and D.O. Tarazano, *A Proposed Form for the Atmospheric Microtemperature Spatial Spectrum in the Input Range*, Private Communication.

34. Site Testing for the VLT. VLT Report No. 60 Munchen. ESO, 1990.

35. V.P. Lukin and V.V. Pokasov, Appl. Opt. **20**, No. 1, 121–135 (1981).

36. A.I. Kon, Izv. Vyssh. Uchebn. Zaved., Ser. Radiofiz. **13**, No. 1, 61–70 (1970).

37. V.P. Lukin, V.M. Sazanovich, and S.M. Slobodyan, Izv. Vyssh. Uchebn. Zaved., Ser. Radiofiz. **23**, No. 6, 721–729 (1980).

38. S.M. Gubkin, O.N. Emaleev, V.P. Lukin, et al., Astron. Zh. **60**, No. 4, 789–794 (1983).

39. V.P. Lukin, V.M. Sazanovich, and S.M. Slobodyan, *Propagation of Optical Waves in the Randomly Inhomogenuious Atmosphere* (Nauka, Novosibirsk, 1979), pp. 61–66.

40. V.P. Lukin and V.M. Sazanovich, Izv. Akad. Nauk SSSR, Ser. FAO **14**, No. 12, 996–1000 (1978).

41. A.M. Obukhov, Izv. Akad. Nauk SSSR, Ser. Geofiz. No. 9, 17–21 (1960).

42. O.N. Emaleev, V.P. Lukin, et al., in: *Abstracts of Reports at the 5th All–Union Symposium on Laser Beam Propagation in the Atmosphere,* Tomsk (1979), Vol. 2, pp. 144–147.